



HAL
open science

Experimental focusing dam break problem in a non-local optical stochastic Kerr medium

A. Aleksanyan, H. Louis, Jean-François Henninot, E. Louvergneaux

► To cite this version:

A. Aleksanyan, H. Louis, Jean-François Henninot, E. Louvergneaux. Experimental focusing dam break problem in a non-local optical stochastic Kerr medium. *Physical Review E*, 2021, 103 (2), 10.1103/PhysRevE.103.022701 . hal-03132375

HAL Id: hal-03132375

<https://hal.science/hal-03132375v1>

Submitted on 27 Nov 2023

HAL is a multi-disciplinary open access archive for the deposit and dissemination of scientific research documents, whether they are published or not. The documents may come from teaching and research institutions in France or abroad, or from public or private research centers.

L'archive ouverte pluridisciplinaire **HAL**, est destinée au dépôt et à la diffusion de documents scientifiques de niveau recherche, publiés ou non, émanant des établissements d'enseignement et de recherche français ou étrangers, des laboratoires publics ou privés.

Experimental focusing dam break problem in a non-local optical stochastic Kerr medium

A. Aleksanyan,¹ H. Louis,¹ J.F. Heninot,² and E. Louvergneaux^{1,*}

¹Univ. Lille, CNRS, UMR 8523 - PhLAM - Physique des Lasers Atomes et Molcules, F-59000 Lille, France

²Univ. Artois, CNRS, UMR 8181 - UCCS - Unite de Catalyse et de Chimie du Solide, F-62307 Lens Cedex, France

(Dated: August 18, 2020)

We experimentally study the propagating of an optical intensity jump discontinuity in a *non-local* stochastic Kerr *focusing* nematic liquid crystal (LC) cell. We show both theoretically and experimentally that non-locality opens a novel route towards beam steering in our system. Indeed, the discontinuity trajectory follows a curve that bends with the injected power. Despite the stochastic nature of the medium and the constant presence of transverse instabilities, the development of a focusing dam-break shock dynamics is shown to survive. The distance Z_s for the *focusing* shock to occur follows a power law with the beam power P according to $Z_s \propto P^\chi$, with $\chi = 4/3$, as for shock dynamics in self-defocusing media.

Any physics student from wave optics class has heard about the phenomenon of diffraction, i.e. varying when wave envelope varies during propagation. They also know that this effect is embedded in Maxwell's equations and the necessary condition for this phenomenon to occur is for the field envelope to depend on the spatial coordinates. This is *linear diffraction*. However an additional term appears in the wave propagation equation if the wave propagates in nonlinear media. This term accounts for the medium polarization and contains the nonlinear part of the index of the medium. If the wave envelope injected into the medium has no transverse spatial dependence (ideal plane wave), no linear diffraction is observed, but diffraction can still occur providing that the nonlinearity varies with space. This is *nonlinear diffraction*. Notion that every physics student has not heard of unless they have pursued a course in nonlinear optics. Thus, there are two cases where an optical beam propagating through a nonlinear medium experiences diffraction, either (i) the initial beam has a structured profile (amplitude or/and phase varying with space) and the nonlinear medium is spatially homogeneous, then the beam linearly diffracts through the nonlinear medium, or (ii) the initial beam is assimilated to a plane wave but the nonlinear medium is spatially structured so that nonlinear diffraction is achieved during propagation (a combination of these two cases is also possible but it is out of the scopes of this study). The nonlinear diffraction was first introduced and evidenced by Isaac Freud in a seminal work using the spatially periodic modulation of the dielectric susceptibility of NH₄CL [1]. Such material structuring will be later implemented for the realization of photonic lattices [2] and lead to novel nonlinear phenomena [3–6]. The most documented studies on nonlinear optical propagation deal with the above-mentioned first situation, that is, an initial beam linearly diffracting along the propagation through a spatially homogeneous nonlinear medium. This is the main core of nonlinear optics

for beam propagation and this article belongs to this category.

Competition or rather "cohabitation" between linear diffraction and nonlinearity has been the subject of an extensive amount of publications. Localization through solitary waves [7–9] or self-similar structures [10–12], modulational instability (also called filamentation) [13–15], wave singularities such as vortices [16], shock waves [17–19] or else wave collapse [20, 21] are some of the manifestations of such dynamics. We are interested in the nonlinear propagation of an optical amplitude jump discontinuity (between two uniform values of the initial data) through nonlinear *focusing* media. This problem belongs to the class of Riemann problems [22, 23]. A Riemann problem [24] classically refers to the initial value problem for a transverse uni-dimensional system associated with hyperbolic equations consisting of two constant states with a step at the origin. When the initial wave amplitude is step-like, the terminology dam break (or dam break Riemann problem) is used, in analogy with dam break flows in hydrodynamics. This situation has been extensively studied in shallow water for the regularization of initial discontinuities via the emergence of dispersive shock waves (also known as undular bores) when dissipation is negligible compared to dispersion [25]. These behaviors were later evidenced in nonlinear optics, when the nonlinearity is of *defocusing* type, in temporal systems [26, 27] as well as in spatial ones [18]. However, that dynamics radically changes when the nonlinearity is of *focusing* nature. The equations become elliptic so a shock boundary condition is ill posed, associated with no long-term undular bore solution but modulational instability. In optics, it is predicted that, for a focusing nonlinearity, whose response is non-local, the shock prevails over modulational instability [19] and focusing dispersive dam break flows emerge in the form of an oscillatory structures endowed with characteristics similar to dispersive shock waves [28]. Wan *et al.* experimentally demonstrated in local focusing media that using a partially-coherent beam suppresses modulational instability but leads to modulations as spatial dispersive shock waves with negative

* eric.louvergneaux@univ-lille.fr

pressure [29]. Thus, there is scant publications and almost no experimental study of the *focusing* dam break problem for an optical beam propagating through *focusing* nonlinear nonlocal media. This is the motivation of this study.

Our experimental setup follows the same strategy as presented in [14]. A step-like intensity beam profile is injected into a transverse unidimensional LC cell (Fig. 1). Such a Heaviside-like profile is prepared by focusing the Gaussian beam by a cylindrical lens (CYL) onto a thin metallic blade with a sharp edge. A $4f$ imaging system is constructed via two $f = 100\text{ mm}$ lenses (L) to image the light profile from the plane Σ of the cutter (C) to the entrance plane Σ' of the LC cell. The cell is mounted on a 3D stage and additional rotating stages allowing for precise adjustments via translations and rotations in any direction. To ensure that there is no pre-propagation in air at the cell entrance, a series of videos of the injected probe beam are recorded for different locations z of the cell. These videos are averaged over 20 s acquisition time to reveal the possible air diffraction pattern and adjust the entrance of the cell Σ' with the plane Σ of the cutter. The single-mode frequency doubled $Nd^{+3} : YVO_4$ ($\lambda_0 = 532\text{ nm}$) laser with electric field A is linearly polarized along the x -axis initially perpendicular to the extraordinary axis of LC molecules. The input laser beam radii at the entrance of the cell, measured via a camera beam profiler (Thorlabs BC106N-VIS/M), are $\omega_x \approx 11.5\ \mu\text{m}$ and $\omega_y \approx 960\ \mu\text{m}$ (in the cutter plane). Thus, no more than one filament can form in the vertical x direction. The nonlinear medium is a E7 nematic LC of $75\ \mu\text{m}$ thickness sandwiched between two glass substrates with planar (parallel to the walls) anchoring conditions. The entrance of the cell is closed by a glass substrate with a planar anchoring condition to avoid depolarizing effects during beam injection. A white light imaging system (WL+IS1 on Fig. 1) is constructed to image the plane Σ' along with the injected one-dimensional beam profile insuring that the latter is parallel to the walls of

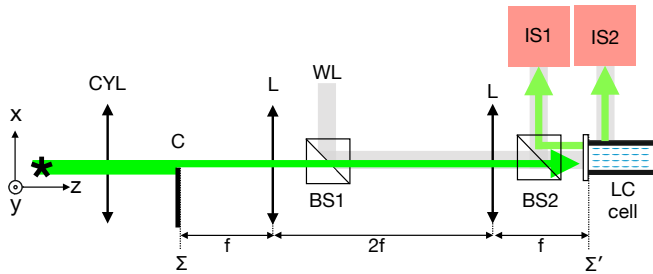


FIG. 1. Experimental setup: CYL - cylindrical lens with $f = 75\text{ mm}$ focal length, C - light cutter, L - plano-concave lenses with $f = 100\text{ mm}$ focal length, BS1, BS2 - beam splitters. IS1 - imaging system composed of a 10X, NA = 0.25 microscope objective (Olympus) and a camera (Thorlabs CMOS camera, 10bit). BS2 - an imaging system composed of a 5X, NA = 0.1 microscope objective (Mitutoyo) mounted on a lens tube with $f = 200\text{ mm}$ focal length and a camera (Thorlabs).

the LC cell. The propagation evolution of the beam is tracked via imaging system IS2 using the scattered light in the x direction. The propagating optical field is scattered by LC molecule fluctuations depending on director axis orientation, input field polarization and observation direction [30, 31]. It is not a direct image of the optical field but of its scattering by the refractive index profile. However, as in all studies on optical beam propagation through nematic LCs, it allows for qualitative analysis of the dynamics.

The model describing the nonlinear propagation dynamics in such complex media is governed by a system of coupled equations for the optical reorientation angle θ of the LC molecules and the light envelope amplitude A [32], such as

$$\gamma \frac{\partial \theta}{\partial t} = K_2 \frac{\partial^2 \theta}{\partial y^2} + C_{1T} A^2 \sin(2\theta) + \sqrt{\epsilon} \xi \quad (1)$$

$$0 = -2ik_0 n_{\perp} \frac{\partial A}{\partial z} + \frac{\partial^2 A}{\partial y^2} + k_0^2 n_a^2 \sin(\theta)^2 A + ik_0 n_{\perp} \beta A, \quad (2)$$

where γ is viscosity, K_2 is the Frank's twist elastic constant, $n_a = n_{\parallel} - n_{\perp}$ is the optical anisotropy with n_{\parallel}/n_{\perp} being the extraordinary/ordinary indices, $C_{1T} = \epsilon_0 n_a^2/4$, k_0 is the laser wavenumber and β are losses. ϵ is the intensity of the thermal noise source term ξ which is Gaussian and delta correlated [33]. At third order in θ , dimensionless form of Eqs.(1,2) is

$$\begin{cases} \frac{\partial \psi}{\partial T} = \sigma_0^2 \frac{\partial^2 \psi}{\partial Y^2} + 2|a|^2 \psi + \sqrt{\eta} \xi \\ i \frac{\partial a}{\partial Z} = \frac{1}{2} \frac{\partial^2 a}{\partial Y^2} + \frac{1}{C_a^2} \psi^2 a + i \frac{\alpha}{2} a \end{cases} \quad (3)$$

where following scalings are introduced: optical field A with respect to the optical Fredericksz threshold is scaled

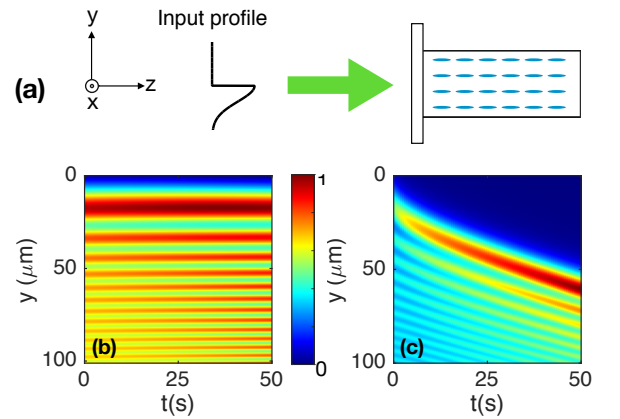


FIG. 2. (a) Step-like Gaussian intensity profile injected in the LC cell. Spatiotemporal evolution of the beam transverse profile after $z = 1.2\text{ mm}$ propagation for (b) the local ($K_2 = 0$) and (c) non-local ($K_2 = 6.57 \cdot 10^{-12}\text{ N}$) cases. Both profiles are normalized to their maximum values. (b) $A = 5000$ and (c) $A = 31250$. $\epsilon = 0$, $\beta = 0$, $n_{\parallel} = 1.7589$, $n_{\perp} = 1.5269$, $\lambda_0 = 532 \cdot 10^{-9}\text{ m}$ and $\omega_y \approx 960\ \mu\text{m}$.

as $A_{Fr} = \pi/L\sqrt{K_3/C_{1T}}$, such that $a = A/A_{Fr}$, L being the cell thickness and K_3 the bend elastic constant. $Y = y/(\sqrt{2}w_y)$, $Z = z/(2k_0n_\perp w_y^2)$, $T = tK_3\pi^2/(\gamma L^2)$, $\psi = \theta w_y^2 k_0^2 n_a^2$. $\alpha = 2k_0n_\perp w_y^2 \beta$, $C_a = w_y^2 k_0^2 n_a^2$, $\sqrt{\eta} = \sqrt{\varepsilon L^2 C_a/(\pi^2 K_2)}$. $\sigma_0 = \frac{L}{\pi w_y} \sqrt{\frac{K_2}{2K_3}}$ accounts for the degree of non-locality.

It is worth to mention that such a system of equations Eq. (3), even for stationary, deterministic and lossless conditions, is fundamentally different from the local nonlinear Schrödinger equation usually referred to study dam break problems in optics [23, 29] as well as in hydrodynamics [22], hence, different dynamics is anticipated.

Fig. 2(b) depicts the spatio-temporal evolution of the y -transverse profile of the optical intensity $|A|^2$ after $z = 1.2 \text{ mm}$ propagation for Eqs.(1,2) in the *local limit*, that is $K_2 = 0$, without noise nor losses ($\epsilon = 0$ and $\beta = 0$) and for an initial amplitude value of the optical field at $z = 0$ leading to focusing dam break shock. An oscillatory wave regularizing the discontinuity is clearly evidenced. Its evolution with time stays stationary even at the early stage of the dam break (as also visible in [29]). On the contrary, taking into account for the non-local response of the nonlinearity ($K_2 = 6.57 \cdot 10^{-12} N$) gives a radically different dynamics [Fig. 2(c)]. The oscillatory wave regularizing the discontinuity still remains but its leading edge drifts with time to the highest intensity side. The whole transverse structure is steered during the propagation to the highest intensity value by more than $50 \mu\text{m}$ in the example of Fig. 2(c). Thus, all-optical beam-steering is observed owing to the non-local nature of our system.

Experimentally, (i) the intrinsic thermal fluctuations are known to affect the dynamics [33] and (ii) the scattering losses are relatively high ($\beta \sim 600 \text{ m}^{-1}$), so we expect competition between shock dynamics and filamentation (absent in the ideal case of simulations depicted in Fig. 2) as pointed out in [19, 28] and wonder if shock dynamics can still survive in our stochastic system. Since diffraction and dissipation (scattering losses) are present, we also question on the type of regularization mechanism for shock dynamics that can occur.

Typical experimental propagation evolution of the initial optical intensity jump discontinuity with increasing nonlinearity is displayed on Fig. 3(a-c). The dynamics exhibits a continuous evolution of the fine structure of the propagating optical pattern due to the stochastic nature of the nonlinear medium as described in [34]. However, its global shape remains quasi-stationary after a transient set up time. Thus, videos of the dynamics are recorded (20 s duration at 5 fps) with a 10 bit depth dynamic range to extract corresponding averaged images representative of the global shape of the propagating structure as presented on Fig. 3(a-c). The acquisition time of the camera is automatically adjusted by the software to get unsaturated videos taking into account eventual light pinning or saturated pixels due to cell impurities. The first $200 \mu\text{m}$ of propagation are not reported on experimental plots (i)

to avoid scattered signals from the optical field injection at the entrance of the cell and mainly (ii) to allow for the input light to transfer its boundary condition discontinuity on the LC molecule distribution, that is to the medium refractive index. This latter point is crucial since our system is described by a set of two coupled equations [Eqs.(1,2)] and the initial boundary condition is only applied to the light envelope amplitude A , not to the optical reorientation angle θ of the LC molecules. In usual setups where the dam break Riemann problem is studied, only one variable accounts for the propagation dynamics of the system (e.g. nonlinear Schrödinger equation or Kortewegde Vries equation) and the initial

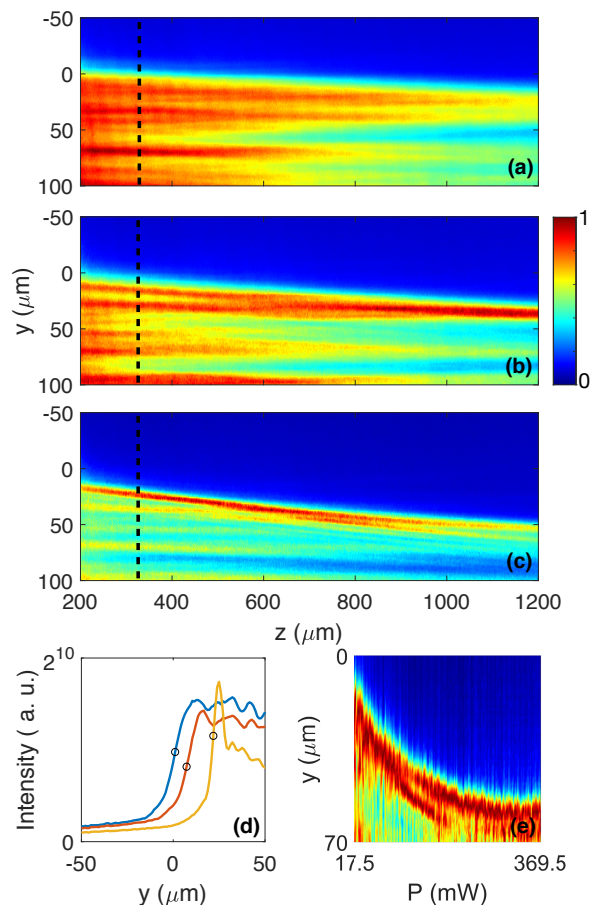


FIG. 3. Spatial evolution of the initial intensity jump discontinuity versus propagating distance z for increasing laser power measured before the sample entrance, namely (a) $P = 17.5 \text{ mW}$, (b) $P = 73.8 \text{ mW}$ and (c) $P = 193.5 \text{ mW}$. The intensity profiles are normalized to their maximum values. (d) Transverse intensity profiles at $z = 354 \mu\text{m}$ propagating distance [dotted lines on (a), (b) and (c)] for the three power values of diagrams (a), (b) and (c). Black circles on (d) locate the scattered light intensity discontinuity Y_S (see text for definition). (e) Evolution of the intensity profile at $z = 1200 \mu\text{m}$ versus the injected light power P ; the transverse profiles collected for each value of P are normalized to 1 in order the render the image readable. All data are averaged over 20 seconds of dynamics.

condition is applied to this variable [27, 35, 36]. Also, the scattered light recorded by the camera IS2 is a result of the LC index distribution that has no initial jump discontinuity at $z = 0$ but will only acquire it over the early stage of propagation ($100 - 200 \mu\text{m}$).

Three values of the injected optical power P , representative of the dynamics of interest, are shown on Fig. 3(a-c), namely $P = 17.5 \text{ mW}$, $P = 193.5 \text{ mW}$, and $P = 286.7 \text{ mW}$. For the lowest power [Fig. 3(a)] the regime is dominated by linear diffraction and observed small deviation experienced by the discontinuity is attributed to linear Fresnel diffraction. The dynamics drastically changes when increasing the laser power with a transverse shift of the sharp edge [Fig. 3(b,c)]. The edge steering is clearly evidenced on Fig. 3(d) through the transverse intensity profiles plotted at a fixed propagation distance, namely $z = 354 \mu\text{m}$, for the three powers of Fig. 3(a-c). A shift of $\sim 20 \mu\text{m}$ is obtained after only $354 \mu\text{m}$ propagation. The 0 reference of the transverse y -axis is fixed by the location of the discontinuity at $z = 200 \mu\text{m}$ in the linear regime (that is $P = 17.5 \text{ mW}$). Fig. 3(d) also evidences the steepening of the edge with increasing the power. For the highest depicted power [Fig. 3(c)], the reached transverse steering at 1.2 mm propagation distance from the cell entrance is at least $40 \mu\text{m}$, that is a larger than 33 mrad . The amount of steering obtained after 1.2 mm propagation versus the input beam power P is plotted on Fig. 3(e) clearly demonstrating a power dependence of the sharp edge position shift. For a quantitative analysis of this nonlinear beam deviation, the transverse position Y_s of the intensity discontinuity is tracked. As an example, Y_s is marked by a black circle on profiles of Fig. 3(d). At a given propagating distance z , Y_s corresponds to the abscissa of the maximum of the transverse intensity steepness calculated as $S_z(y) = (\partial|A|^2/\partial y)|_z$. The measurement of this dependence brings out a power law for Y_s as depicted on Fig. 4(d), namely $Y_s \propto P^{\frac{1}{25}}$.

Experimental results of Fig. 3 show that the beam steering predicted in Fig. 2 is a robust phenomenon with respect to noise and scattering losses. On the other hand, Fig. 3 does not allow for the evidence of focusing dispersive dam break flows in the form of an oscillatory structure as evidenced in Fig. 2(b,c). A numerical study would be necessary to identify the effects of noise, losses and e.g. nonlinearity saturation effects on the emergence of the focusing dispersive oscillating structure. This is out of the scope of this letter since the high transverse spatial resolution required to perform numerical simulations on a such wide beam profile requires many weeks of computing to reach the stationary state in the deterministic case. This is why in this letter we do not directly contrast our experimental results with numerical ones, based on Eqs.(1,2). Transverse instabilities, in the form of modulational instabilities, starting from the early stage of propagation (so not the focusing dispersive dam break flows expected as a result of the regularization of the discontinuity) are always present even

for the "linear regime" of Fig. 3(a) as mentioned in [37]. The averaged pictures of Fig. 3(a-c) do not emphasize them since their transverse location and periodicity are wandering with time [34] and are washed out by the averaging process. Further study would be necessary to identify these short wavelength instabilities with noise sustained modulational instability [14] or other stochastic resonance behavior [38]. Although no focusing dispersive dam break flows are experimentally observed in our stochastic nonlinear medium, shock-like dynamics is still observable. Focusing dam-break shock results from the underlying mechanism of the wave steepening driven by the nonlinearity which leads to a gradient catastrophe. The self-steepening dynamics of our experimental refractive index discontinuity is analyzed versus the propagation using the previously defined steepness $S_z(y)$. For each z , the maximum value S_{max_z} of $S_z(y)$ is extracted. The typical experimental evolution, during the propagation, of the maximum transverse steepening $S_{max_z}(z)$ for the discontinuity between the ground and high intensity regions, versus power injection P is illustrated in Fig. 4(a). The plotted $S_{max_z}(z)$ profiles correspond to the average of the 100 instantaneous steepness profiles extracted from each frame of the video. In order to avoid noise-induced hot spots and small scale transverse instabilities in the calculation of S , Savitzky-Golay algorithm is applied to smooth the signal. It is observed that above $P \approx 135 \text{ mW}$ power, the evolution of $S_{max_z}(z)$ always reveals the occurrence of a maximum (Fig. 4(a)). It indicates that the jump distribution of the index profile self-steepens during the propagation distance z before "relaxing" or being "regularized" by the dispersive and dissipative medium. This is the characteristics of a shock-like dynamics. Such observation is also reported by Wan *et al.* [29] for the diffraction from an edge but in a *local self-focusing* medium.

Steepness oscillations S_{max_z} along the propagation direction are linked to the corresponding transverse oscillations on the intensity profiles [Fig. 3(d)]. This feature is found in the numerical simulations carried out without noise nor losses ($\epsilon = 0$ and $\beta = 0$) but taking into account for the non-local response of the nonlinearity ($K_2 = 6.57 \cdot 10^{-12} \text{ N}$) [Fig. 4(b)]. These oscillations come from the transverse modulations previously discussed [Fig. 3(a-c)] and their interactions due to the non-locality. The location of $S(z)$ maximum never occurs above approximately $600 \mu\text{m}$ propagating distance. The reason is certainly due to losses that overcome nonlinearity for this distance. Such a limitation in the nonlinear effects was already reported in [34]. We extract the longitudinal coordinate Z_s corresponding to the maximum value of $S_{max_z}(z)$ that measures the propagating distance needed for the focusing shock-like to occur. This distance Z_s moves towards the cell entrance when increasing the initial beam power P as reported for shocks in optical defocusing media (see e.g. [39]) and in hydrodynamics [19, 20]). Indeed, it is known that the shock distance Z_s scales with power P according to the law $Z_s \propto P^X$, with

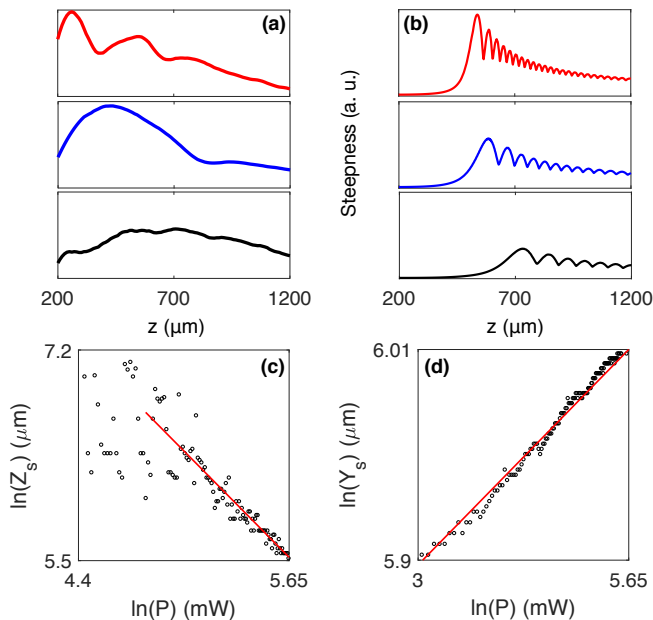


FIG. 4. (a) Typical experimental maximum transverse steepening $S_{max_z}(z)$ (see text for definition) evolution with increasing power, $P = 137.18 \text{ mW}$ (black), 193.5 mW (blue), and 279.7 mW (red); the dot indicates the location Z_s and refers to the maximum of $S_{max_z}(z)$. (b) Numerical maximum transverse steepening $S_{max_z}(z)$ evolution with increasing intensity values $|A|^2 = 5.64 \cdot 10^6$ (black), $|A|^2 = 7.98 \cdot 10^6$ (blue) and $|A|^2 = 9.76 \cdot 10^6 \text{ V}^2/\text{m}^2$ (red) correspondingly. (c) Experimental evolution of the focusing shock-like distance Z_s (see text for definition) versus injected power P in logarithmic scales showing a power law $Z_s \propto P^\chi$, with $\chi = -4/3$ coefficient. (d) Experimental evolution of the transverse position Y_s of the intensity discontinuity (see text for definition) at $z = 1.2 \text{ mm}$ versus injected power P in logarithmic scales showing a power law $Y_s \propto P^\chi$, with $\chi = 1/25$ coefficient. All experimental values are averaged over 20 seconds of dynamics.

$\chi = 0.5$ in the hydrodynamic limit. The evolution plot of Z_s versus P for our experimental recordings is drawn on Fig. 4(c). It clearly evidences a power law $Z_s \propto P^{4/3}$ for powers larger than $P \approx 135 \text{ mW}$ ($\ln(P) \approx -4.9$). Thus, as for shocks in defocusing media a power law in the form of $Z_s \propto P^\chi$ is found. Our $\chi = 4/3$ value is related to the non-local nature of our system as shown by Conti *et al.* and Ghofrahina *et al.* in [20, 39]. A numerical study would state on the influence of the level of non-locality on the χ parameter in our system.

In conclusion, we experimentally show that the propagation of an optical intensity jump discontinuity (dam break problem) in a *non-local focusing* Kerr medium follows a trajectory that bends with the injected beam power P due to the non-local nature of the nonlinearity. The transverse beam nonlinear deviation/shift Y_s follows a power law with $Y_s \propto P^{1/25}$. This opens a novel all-optical route towards beam steering. We also evidenced that the profile of the refractive index self-steepens along propagation and leads to a focusing shock dynamics. It is characterized by a power law, as for self-defocusing local Kerr media, for the shock distance to occur versus the injected beam power P , namely $P^{-4/3}$. Focusing dispersive dam break oscillatory structure, that results from the regularization of the shock, is not observed due to the intrinsic noise that sustains wandering small scale transverse instabilities. Further investigations are in progress to blackuce the stochasticity level in order to evidence experimentally focusing dispersive dam break flow or maybe dissipative one due to losses.

-
- [1] I. Freund, Nonlinear Diffraction, Phys. Rev. Lett. **21**, 1404 (1968).
- [2] J. D. Joannopoulos, P. R. Villeneuve, and S. Fan, Photonic crystals putting a new twist on light, Nature **386**, 143 (1997).
- [3] D. Gomila, R. Zambrini, and G.-L. Oppo, Photonic band-gap inhibition of modulational instabilities, Phys. Rev. Lett. **92**, 253904 (2004).
- [4] U. Peschel, O. Egorov, and F. Lederer, Discrete cavity solitons, in *Nonlinear Guided Waves and Their Applications* (Optical Society of America, 2004) p. WB6.
- [5] S. Koke, D. Träger, P. Jander, M. Chen, D. N. Neshev, W. Krolikowski, Y. S. Kivshar, and C. Denz, Stabilization of counterpropagating solitons by photonic lattices, Opt. Express **15**, 6279 (2007).
- [6] N. Marsal, D. Wolfersberger, M. Sciamanna, G. Montemezzani, and D. N. Neshev, Experimental control of pattern formation by photonic lattices, Opt. Lett. **33**, 2509 (2008).
- [7] B. Schapers, M. Feldmann, T. Ackemann, and W. Lange, Interaction of localized structures in an optical pattern-forming system, Phys. Rev. Lett. **85**, 748 (2000).
- [8] S. Barland, J. Tredicce, and M. Brambilla, Cavity solitons as pixels in semiconductor microcavities, Nature **001588**, 699 (2002).
- [9] A. Piccardi, A. Alberucci, N. Tabiryan, and G. Assanto, Dark nematicons, Opt. Lett. **36**, 1356 (2011).
- [10] A. W. Snyder and J. Mitchell, Accessible Solitons, Science **276**, 1538 (1997).
- [11] D. Buccoliero and A. S. Desyatnikov, Quasi-periodic transformations of nonlocal spatial solitons, Opt. Express **17**, 9608 (2009).
- [12] A. Alberucci, C. P. Jisha, and G. Assanto, Breather solitons in highly nonlocal media, J. Opt. **18**, 125501 (2016).
- [13] G. A. El', A. V. Gurevich, V. V. Khodorovski, and A. L. Krylov, Modulational instability and formation of a nonlinear oscillatory structure in a "focusing" medium, Phys. Lett. A **177**, 357 (1993).
- [14] M. Peccianti, C. Conti, and G. Assanto, Optical modulational instability in a nonlocal medium, Phys. Rev. E

- 68**, 025602(R) (2003).
- [15] W. Królikowski, O. Bang, N. I. Nikolov, D. Neshev, J. Wyller, J. J. Rasmussen, and D. Edmundson, Modulational instability, solitons and beam propagation in spatially nonlocal nonlinear media, *J. Opt. B* **6**, S288 (2004).
- [16] Y. V. Izdebskaya, V. G. Shvedov, P. S. Jung, and W. Krolikowski, Stable vortex soliton in nonlocal media with orientational nonlinearity, *Opt. Lett.* **43**, 66 (2018).
- [17] M. A. Hofer, M. J. Ablowitz, I. Coddington, E. A. Cornell, P. Engels, and V. Schweikhard, Dispersive and classical shock waves in bose-einstein condensates and gas dynamics, *Phys. Rev. A* **74**, 023623 (2006).
- [18] W. Wan, S. Jia, and J. W. Fleischer, Dispersive superfluid-like shock waves in nonlinear optics, *Nature Physics* **3**, 46 (2007).
- [19] N. Ghofraniha, C. Conti, G. Ruocco, and S. Trillo, Shocks in Nonlocal Media, *Phys. Rev. Lett.* **99**, 043903 (2007).
- [20] C. Conti, A. Fratolocci, M. Peccianti, G. Ruocco, and S. Trillo, Observation of a gradient catastrophe generating solitons, *Phys. Rev. Lett.* **102**, 083902 (2009).
- [21] M. Bertola and A. Tovbis, Universality for the Focusing Nonlinear Schrödinger Equation at the Gradient Catastrophe Point: Rational Breathers and Poles of the Tricritical Solution to Painlevé I, *Commun. Pure Appl. Math* **66**, 678 (2013).
- [22] G. A. El and M. A. Hofer, Dispersive shock waves and modulation theory, *Physica D* **333**, 11 (2016).
- [23] G. Biondini, Riemann problems and dispersive shocks in self-focusing media, *Phys. Rev. E* **98**, 052220 (2018).
- [24] B. Riemann, Über die fortpflanzung ebener luftwellen von endlicher schwingungsweite, *Abhandl. König. Gesell. Wiss., Göttingen* **8**, 43 (1860).
- [25] D. H. Peregrine, Calculations of the development of an undular bore, *J. Fluid Mech.* **25**, 321 (1966).
- [26] J. Fatome, C. Finot, G. Millot, A. Armaroli, and S. Trillo, Observation of optical undular bores in multiple four-wave mixing, *Phys. Rev. X* **4**, 021022 (2014).
- [27] G. Xu, M. Conforti, A. Kudlinski, A. Mussot, and S. Trillo, Dispersive Dam-Break Flow of a Photon Fluid, *Phys. Rev. Lett.* **118**, 254101 (2017).
- [28] G. Assanto, T. R. Marchant, and N. F. Smyth, Collisionless shock resolution in nematic liquid crystals, *Phys. Rev. A* **78**, 063808 (2008).
- [29] W. Wan, D. V. Dylov, C. Barsi, and J. W. Fleischer, Diffraction from an edge in a self-focusing medium., *Opt. Lett.* **35**, 2819 (2010).
- [30] P. de Gennes and J. Prost, *The physics of liquid crystal* (Oxford University Press Inc., New York, 1993).
- [31] I. C. Khoo, *Liquid crystals, Physical Properties and Nonlinear Optical Phenomena* (Wiley-Interscience, New York, 1995).
- [32] X. Hutsebaut, C. Cambournac, M. Haelterman, J. Beeckman, and K. Neyts, Measurement of the self-induced waveguide of a solitonlike optical beam in a nematic liquid crystal, *J. Opt. Soc. Am. B* **22**, 1424 (2005).
- [33] G. Agez, C. Szwaj, E. Louvergneaux, and P. Glorieux, Noisy precursors in one-dimensional patterns, *Phys. Rev. A* **66**, 063805 (2002).
- [34] H. Louis, M. Tlidi, and E. Louvergneaux, Experimental evidence of dynamical propagation for solitary waves in ultra slow stochastic non-local Kerr medium, *Opt. Express* **24**, 16206 (2016).
- [35] N. J. Zabusky and M. D. Kruskal, Interaction of Solitons in a Collisionless Plasma and the Recurrence of Initial States, *Phys. Rev. Lett.* **15**, 240 (1965).
- [36] S. Trillo, M. Klein, G. F. Clauss, and M. Onorato, Observation of dispersive shock waves developing from initial depressions in shallow water, *Physica D* **333**, 276 (2016).
- [37] J. Wang, J. Chen, J. Liu, Z. Wang, Y. Li, Q. Guo, W. Hu, and L. Xuan, Observation of Optical Solitons and Abnormal Modulation Instability in Liquid Crystals with Negative Dielectric Anisotropy, arXiv:1503.01953v1.
- [38] X. Feng, H. Liu, N. Huang, Z. Wang, and Y. Zhang, Reconstruction of noisy images via stochastic resonance in nematic liquid crystals, *Sci. Rep.* **9**, 3976 (2019).
- [39] N. Ghofraniha, L. S. Amato, V. Folli, S. Trillo, E. DelRe, and C. Conti, Measurement of scaling laws for shock waves in thermal nonlocal media, *Opt. Lett.* **37**, 2325 (2012).